

Wind loads for high-solidity open-frame structures

Samuel D. Amoroso*^{1a} and Marc L. Levitan^{2b}

¹ENGENSUS,LLC, 9191 Siegen Lane, Building 6, Suite A, Baton Rouge, LA 70810, USA

²Civil and Environmental Engineering Department, Louisiana State University,
3418 Patrick F. Taylor Hall, Baton Rouge, LA 70803, USA

(Received January 1, 2010, Accepted March 27, 2010)

Abstract. Open frame structures, such as those commonly found in industrial process facilities, are often densely occupied with process related equipment. This paper presents a method for estimating wind loads for high-solidity open frame structures that differs from current approaches, which accumulate wind load contributions from various individual structure components. The method considers the structure as a porous block of arbitrary plan dimension that is subject to wind from any direction. The proposed method compares favorably with wind tunnel test results for similar structures. The possibility of defining an upper bound force coefficient is also discussed.

Keywords: open frame structures; wind load; porous structure; force coefficient.

1. Introduction

Open frame structures are common in the process industries. There are established methods available to estimate wind loads for open frame structures (ASCE 2006, ASCE 1997). Although these methods were originally developed for lattice towers and unclad building frames, which often do not have the internal equipment, ductwork, and piping that are common in the process industries, they have been extended for use in such applications. The basis of these methods is a summation of the contributions to the wind load for separate components of the system (such as framing and equipment), taking into account aerodynamic interaction effects among the different components. This approach works well for relatively open (i.e., low solidity) structures. However, as the overall solidity of a structure and equipment increases, not only do the methods become more cumbersome, but their accuracy may be diminished as the simple, empirical understanding of the aerodynamic interaction effects among the framing and equipment becomes insufficient.

This paper examines the wind loads for more solid open frame structures from a different perspective. Rather than accounting for the effects of the various components, the approach here is to relate the force coefficient to variables which describe the overall geometry of the frame/equipment system. The frame and equipment together are treated as a generally rectangular body

* Corresponding Author, Principal Engineer, E-mail: sam.amoroso@engensus.com

^aPrincipal Engineer

^bAssociate Professor

with some degree of porosity. As such, the presumption of an understanding of the flow field effects among the various individual system components is abandoned, and the force coefficient for the entire system is estimated as a whole. This paper briefly reviews literature relevant to the problem, presents an analytical basis for describing wind loads on three-dimensional porous bodies, and examines the relationships between existing wind tunnel data and relevant geometric variables. The possibility of estimating a reasonable upper bound force coefficient is also discussed.

2. Literature review

Darcy's Law is a method of describing the resistance to flow through porous media. This resistance is characterized by the pressure drop that occurs over the flow length. The pressure drop is related to physical characteristics of the flow, including the velocity, the dynamic viscosity of the fluid, the length of the flow path, and an empirically derived permeability index. Darcy's Law is appropriate for flows in which inertial effects are negligible. This is generally the case when the flow under consideration is occurring in a microscopically porous medium such as soil or rock. The Forchheimer equation (Andrade *et al.* 1999) accounts for inertial effects in flows through porous media of more generic scales

$$-\frac{\Delta P}{L} = \alpha \cdot \mu \cdot V + \beta \cdot \rho \cdot V^2 \quad (1)$$

where

V = flow velocity,

μ = dynamic viscosity of fluid,

ΔP = pressure drop,

L = length of flow path,

α = the inverse of the permeability index, and

β = empirically derived inertial parameter,

Using an approach such as Darcy's Law or its modification as the Forchheimer Equation is of limited utility in estimating the wind loads on petrochemical structures for two reasons: first, all of the flow is considered to pass through the porous medium, but for a three dimensional structure, flow will increasingly be diverted around the body's boundaries as the resistance to through flow increases, and second, Eq. (1) is really no different than the definition of an empirical pressure coefficient for cases in which inertial effects are dominant.

Much of the literature regarding the aerodynamics of porous structures is related to perforated plates, porous fences or wind-driven building ventilation. Cook (1990) addressed the balance of flow through and around porous plates by comparing the process to the principle of minimum strain energy from mechanics. Cook describes theoretical attempts to define the combination of flows around and through a body but concludes that it is necessary to resort to empiricism.

Richards and Robinson (1999) studied wind loads on porous structures, by which they referred to single planes of screens or fences. By interpreting various theoretical considerations in light of both full-scale and wind tunnel experiments, they concluded that loads on these structures are directly proportional to the loads on their solid counterparts by the solidity ratio. They also concluded that the loss coefficient (or drag coefficient) for these structures varied with the angle of wind incidence

at a cosine-squared rate.

Letchford (2001) found that the reduction in force for a porous signboard compared to its solid counterpart occurred at a rate proportional to the 1.5 power of the porosity, rather than the linear rate proposed by Richards and Robinson (1999) or the square rate proposed by the Australian wind loading standard (Standards Australia 2002). In these sources the porosity is the complement of the solidity ratio (i.e., porosity, $p = 1 - \phi$).

Yaragal *et al.* (2002) measured mean flow field characteristics in the wakes of perforated, two-dimensional plates with wake splitters. They found that for plate porosities greater than 30% (or a solidity ratio less than 70%), there was no separation bubble present behind the plate. Furthermore, the character of the pressure deficit in the wake of the plate was distinct for plate porosities above and below this threshold. For porosities less than or equal to 30%, the pressure in the wake continued to decrease for some distance before increasing, whereas the pressure increased monotonically in the wakes of plates with porosities greater than 30%.

Yaragal (2004) measured fluctuating flow properties in the wakes of two-dimensional plates with a range of perforation from 0% (solid plate) to 50%. The variation of RMS pressures and velocities were reported for the different degrees of perforation, and it was found that the magnitudes of these quantities generally decrease as the plates become more highly perforated.

Seifert *et al.* (2006) used a computational fluid dynamics (CFD) approach to study the flow of air through porous buildings with large openings. They found that simplified methods for computing ventilation rates, which related flow rate to the external pressure coefficients and a loss coefficient for the opening, compared well with the more sophisticated CFD results when pairs of openings in the building surface were not aligned with the general flow direction. When the pairs of openings were aligned with the external flow direction, the formation of a coherent stream tube within the model's internal volume increased the flow rate beyond what was predicted by the simplified method.

In an application more closely related to the problem at hand, Cook (1990) offered an empirical relationship describing the relationship between the force coefficient, the wind incidence angle, and the length to width aspect ratio of three-dimensional arrays or frames. The approach was limited to relatively open structures (solidity ratio < 0.3). The form of the equation reflects the fact that the maximum force coefficient for a structural axis occurs for wind directions that are skewed to the structural axes, and this effect increases as the relative along-wind length of the structure increases. The rate at which the force coefficient increases with length/width ratio was given to be the aspect ratio to the 0.8 power.

3. Analytical considerations

Prior to introducing any analytical considerations for the wind loads on dense open frame structures it is necessary to establish sign, and other, conventions for describing the geometry of the system. Fig. 1 is a schematic representation of the plan view of a generic structure. The structure is shown to be rectangular in plan with coordinate axes oriented parallel to the sides of the structure. The side of the structure parallel to the x -axis has length L , and the side parallel to the y -axis has length B . The wind direction is measured with respect to the negative x -axis and is designated α . Some other geometric constructions are also shown in Fig. 1. The angle θ is formed between the side of the structure parallel to the x -axis and the diagonal of the structure. The projected width perpendicular to the wind direction is designated B' . The projected width varies with wind angle

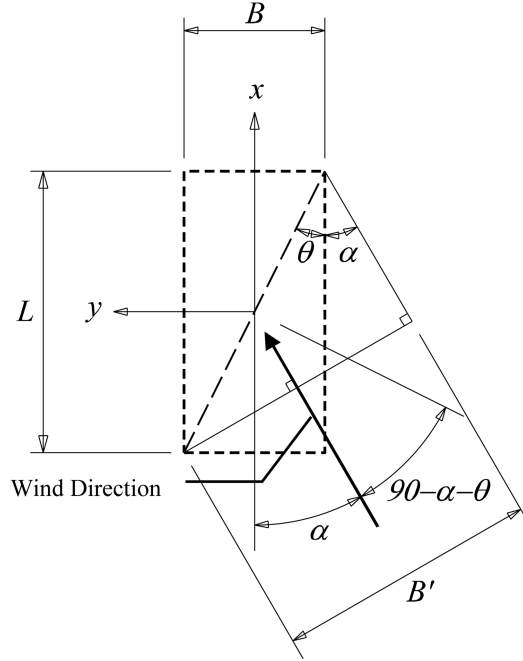


Fig. 1 Schematic plan of a generic rectangular structure showing sign convention and angle convention

such that B' is equal to B when $\alpha = 0$ radians, is equal to $\sqrt{B^2 + L^2}$ when $\alpha = (\pi/2) - \theta$ radians, and is equal to L when $\alpha = \pi/2$ radians.

Having defined the geometry of the system, it is possible to derive mathematical representations for 1) the variation of the force coefficient with wind angle for a given plan coordinate direction, 2) the angle at which the maximum force coefficient occurs, and 3) the value of the maximum force coefficient. Some assumptions are required in order to develop the model. These will be pointed out and explained during the derivation. The angle θ varies with the plan dimensions B and L as follows

$$\theta(B, L) = \tan^{-1}\left(\frac{B}{L}\right) \quad (2)$$

The projected width normal to the wind direction is

$$B'(\alpha, B, L) = \sqrt{B^2 + L^2} \cdot \sin(\alpha + \theta(B, L)) \quad (3)$$

A baseline force coefficient for the structure is defined as a function of the solidity ratio, ϕ , after Letchford (2001)

$$C_1(\phi) = C_0 \cdot (1 - (1 - \phi)^{1.5}) \quad (4)$$

where C_0 is an empirical force coefficient representative of the solid body. A typical value for a rectangular structure may be 1.3, but some discretion or calibration is accommodated by adjusting this value. The solidity ratio is the quotient of the projected area to envelope area normal to the structural axis of interest. It is further assumed that the porosity of the structure is homogeneous,

and therefore, Eq. (4) is approximated at other wind angles. Other functional forms for the change in force coefficient with solidity ratio could be easily substituted if justified. The resulting equation for the variation of the force coefficient along the x -axis with respect to wind angle for a porous body is

$$C_{fx}(\alpha, B, L, \phi) = C_1(\phi) \cdot \frac{B'(\alpha, B, L)}{B} \cdot \cos(\alpha) \quad (5)$$

Eq. (5) represents the fact that the force coefficient for open frame structures almost always increases as α deviates from 0 radians by using a new reference width – the width projected normal to the flow direction. The cosine term reflects the assumption that the x -direction force will diminish as α increases from 0 to $\pi / 2$ radians (0° to 90°). From experience, this assumption is true for homogenous porosity (i.e., the absence of any geometric singularities such as partial cladding or asymmetric arrangement of framing or equipment). The behavior of Eqs. (3) and (5) are illustrated in Fig. 2.

Simply stated, Eq. (5) estimates the component of the along-wind, or drag, coefficient that acts along the x -axis. As the projected width B' increases, so does the drag coefficient. However, as the wind angle deviates from alignment with the x -axis, the component of the drag acting along the x -axis decreases with the cosine function. The development of Eq. (5) assumes that the drag force dominates and the across-wind component of force is negligible. A rationale for the latter assumption is that the chaotic flow field within and around a structure such as the one idealized here would prevent the development of coherent pressure variations in the across-wind direction for the structure as a whole. While individual elements of an open frame structure would be subject to across-wind forces, these effects would cancel one another when considering the aerodynamics of the entire structure.

The angle at which the maximum force coefficient occurs can be calculated by evaluating the first derivative of Eq. (5) with respect to α , setting the result equal to zero, and solving for α .

$$\alpha_{\max}(B, L, \phi) = \tan^{-1}\left(\frac{-B \pm \sqrt{B^2 + L^2}}{L}\right) \quad (6)$$

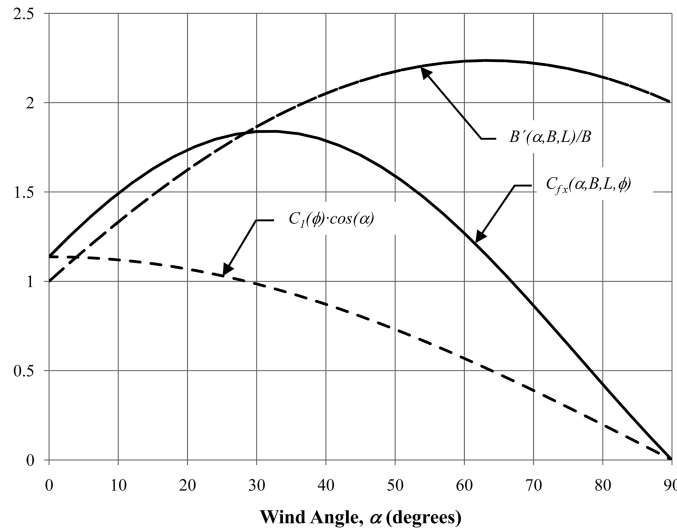


Fig. 2 Variation of the force coefficient of a porous structure with wind angle for $L/B = 2$, $\phi = 0.75$ and $C_0 = 1.3$ according to Eqs. (3) and (5)

Since Eq. (5) has been defined for forces acting along the positive x -direction and for angles, α , between 0 and $\pi / 2$ radians, only one of the solutions for α_{max} is appropriate

$$\alpha_{max}(B, L, \phi) = \tan^{-1}\left(\frac{-B + \sqrt{B^2 + L^2}}{L}\right) \quad (7)$$

The value of α_{max} varies between 0 and $\pi / 4$ (0° and 45°) as the plan aspect ratio, L/B , for the structure increases from 0 to ∞ . Fig. 3 illustrates this variation.

Substitution of Eq. (7) into Eq. (5) yields the following expression for the maximum force coefficient along the x -axis after some simplification

$$C_{fx_max}(B, L, \phi) = \frac{C_0 \cdot (1 - (1 - \phi)^{1.5}) \cdot \sqrt{B^2 + L^2}}{2 \cdot \left(1 + \frac{B^2}{L^2} - \frac{B}{L^2} \cdot \sqrt{B^2 + L^2}\right) \cdot B} \quad (8)$$

Fig. 4 shows how the maximum force coefficient varies with plan aspect ratio, L/B , for porous bodies of three different solidity ratios. It is apparent from the graph that the form of Eq. (8) is hyperbolic, and that the function is basically linear for $L/B > 2$. This infinite increase in force coefficient with length precludes the possibility of defining an upper bound force coefficient for porous, open frame structures of arbitrary dimensions. The possibility of determining an upper bound force coefficient still remains, but only for a given plan aspect ratio, unless the assumed form of Eq. (4) is incorrect and a local maxima for C_l exists between $\phi = 0$ and $\phi = 1.0$.

4. Empirical considerations

This section will examine the measured force coefficients for model structures with relatively high

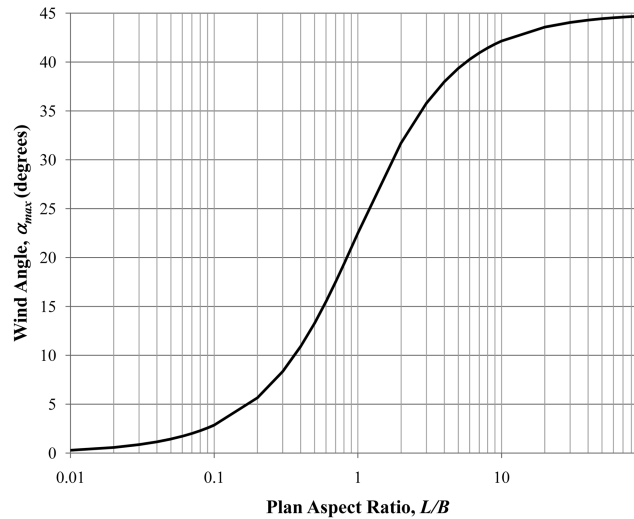


Fig. 3 Variation of α_{max} with plan aspect ratio, L/B (Eq. (7))

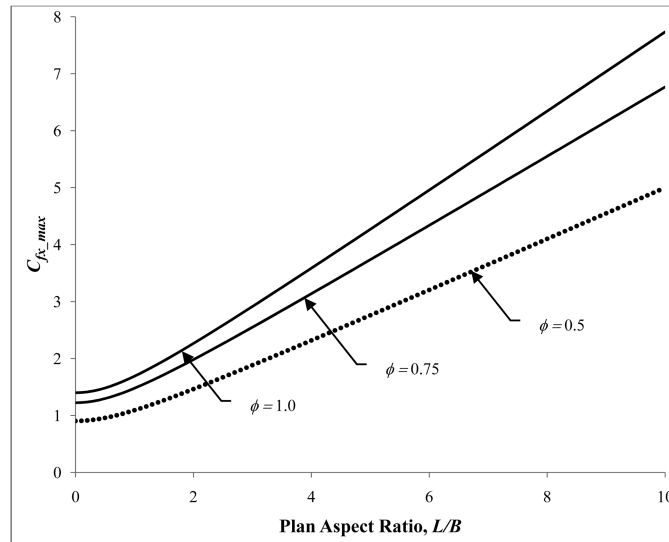


Fig. 4 Variation of maximum force coefficient with plan aspect ratio, L/B , for porous bodies of three different solidity ratios for $C_0 = 1.3$ according to Eq. (8)

solidity ratios in light of the analytical derivation presented in the previous section. The measured force coefficients will also be examined in a purely empirical manner by investigating correlations between the trends in the measurements and combinations of variables that describe the geometry of the structures.

4.1 Comparison of measurements with analytical method

The data for these empirical comparisons are from the wind tunnel measurements reported by Georgiou (1979) and Georgiou and Vickery (1979) on multiple, parallel frames and wind tunnel measurements reported by Qiang (1998) and Levitan *et al.* (2004) on three dimensional models representing open frame structures containing equipment. Since this paper is concerned with higher-solidity structures, only high-solidity subsets of the models that each of these researchers studied have been chosen for the analysis in this section. The seventy-six models chosen from Georgiou's study for this investigation had two different solidity ratios: 0.46 and 0.77. The number of frames among these selected models varied from two to ten, and the spacing to width ratio of the frames within the models varied from 0.095 to 2.045. Georgiou's data were corrected for wind tunnel blockage effects. Thirty-three models were chosen from Qiang's experiments, which had solidity ratios varying from 0.46 to 0.77. Qiang's models had only two frame spacing to width ratios: 0.5 and 0.75. All of Qiang's models had exactly three frames. Qiang's data were not originally corrected for wind tunnel blockage effects, so these corrections have been applied for this study according to the methods described by ESDU (1980). The magnitudes of these corrections were between 8% and 17%.

Fig. 5 shows the variation of the maximum measured force coefficient with respect to the plan aspect ratio, L/B , for all of the selected models from Georgiou and Qiang's experiments. The figure also shows the variation of the maximum force coefficient that is predicted according to Eq. (8) for

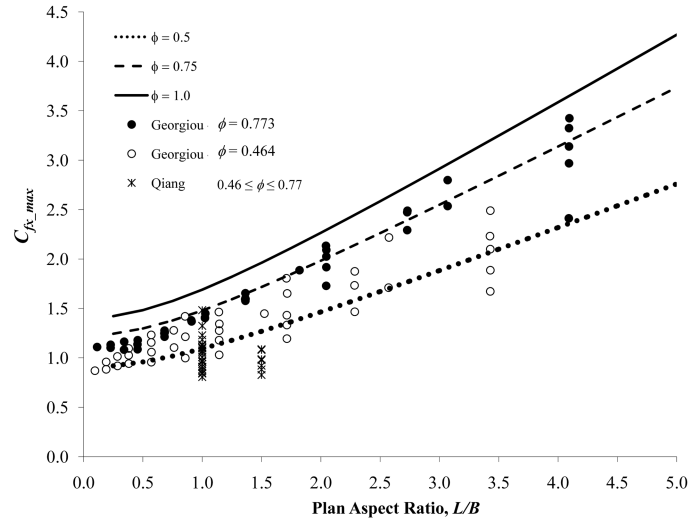


Fig. 5 Variation of maximum force coefficient with plan aspect ratio, L/B , for wind tunnel models and analytical estimates using Eq. (8). C_0 has been set to 1.4 in this figure

three different solidity ratios. It is apparent that the analytical method of Section 2 represents the trends in the data quite well. Georgiou's models with $\phi = 0.77$ generally fall below the lines for $\phi = 0.75$ for the analytical model when L/B is less than 1.0. For larger values of L/B , the data appear to follow the analytical model for $\phi = 0.75$. Georgiou's models with $\phi = 0.46$ generally fall above the line for $\phi = 0.5$ when L/B is less than 1.0. For larger values of L/B , the data appear to be more centered near the analytical model for $\phi = 0.5$. Qiang's measurements, which were for models with $0.46 \leq \phi \leq 0.77$, fall generally below the lines for $\phi = 0.5$ and $\phi = 0.75$ generated by Eq. (8). Qiang's data do not cover a large enough range of aspect ratios to discern whether or not the trend in the analytical model is represented in his measurements.

Fig. 6 illustrates the quality of the correlation between the measured and predicted values of the maximum force coefficient for the selected models. For these calculations the base line force coefficient, C_0 has been set to 1.4. The linear regression through the data has a slope of 0.94 (close to 1.0), and a small intercept, indicating that the Eq. (8) does a reasonable job of capturing the variation in the data. There is scatter in the data, but the correlation coefficient of 0.84 indicates that the model is capturing most of the variation.

It is also useful to examine a few descriptive statistics of the measured and modeled force coefficient values. The predicted values have been divided by the measured values in order to normalize the data set. In this normalized data set, a value of 1.0 indicates that the model perfectly predicted the measured force coefficient, whereas values above or below unity indicate either overestimations or underestimations of the measured values, respectively. For Georgiou and Qiang's models combined, the average value of this parameter is 1.06, indicating that the model systematically overestimates the measured force coefficients. This is no surprise, as it is another way of expressing the slope of the regression line that was discussed in the previous paragraph. The standard deviation of the combined data set is 0.19, and the coefficient of variation is therefore 0.18. The results are different if these same statistics are examined for Georgiou and Qiang's models in isolation. For Georgiou's models, the mean, standard deviation and coefficient of

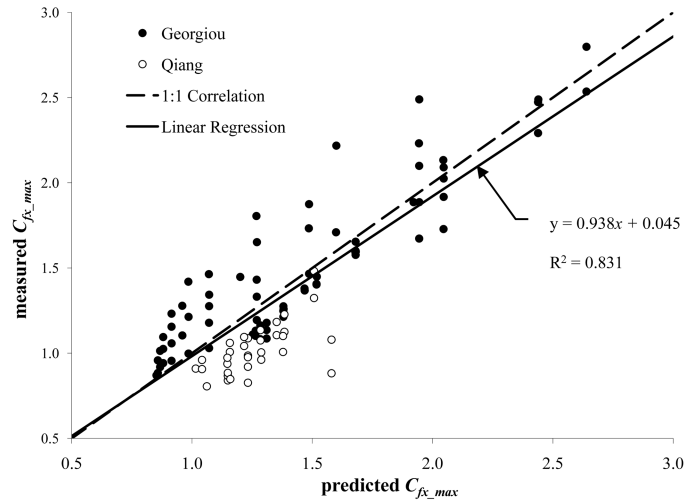


Fig. 6 Measured maximum force coefficients versus maximum force coefficients predicted according to Eq. (8). C_0 has been set to 1.4 for the calculation of the predicted C_f

variation are 0.98, 0.14 and 0.14, respectively. For Qiang's models, these same statistics are 1.25, 0.15 and 0.12. On average, the analytical model more accurately predicts the force coefficients for Georgiou's models. It is possible that the differences in construction of the two sets of models contribute to the differences in the accuracy of the model. The models in Qiang's experiments were fully three dimensional models with two orthogonal frame lines and models of equipment contained inside the frame. Georgiou's models, however, consisted of multiple, parallel plane frames.

4.2 Other empirical considerations

The development of the analytical model in Section 2 identified the solidity ratio and the length to width aspect ratio of a structure as key parameters driving the wind loading force coefficient for relatively dense open frame structures. The comparison of the model's predictions with previous wind tunnel results verifies the importance of these two parameters in the wind loading process for these types of structures. The scatter in the data indicates that there are still other important factors at work in determining the aerodynamic coefficients of the structures. The previous work by Georgiou (1979), Nadeem and Levitan (1997), Qiang (1998) and Levitan *et al.* (2004) have identified a variety of other factors that influence the force coefficient for open frame structures. Among these are the number of frames, the spacing of the frames, the presence or absence of solid flooring, and whether the frames have equal or unequal solidity. In the face of so many variables, it is advantageous to identify a small number of key geometric parameters, each of which is able to encompass multiple variables affecting the force coefficient. This is similar in concept to the process of dimensional analysis in fluid mechanics. Since the assumption of homogeneous porosity in the analytical model of section 2 seemed to be too restrictive in some cases, another useful variable might be one that describes the distribution of solidity within the structure.

Intuitively it seems that for open frame structures with the same envelope geometry, the aerodynamic behavior would differ for cases in which the solidity of the structure was concentrated at the center, evenly distributed throughout, or concentrated at the edges of the structure. This

geometric variation can be described mathematically using the second moment of area. This analytical tool is familiar to engineers when it is used to calculate moments of inertia. Another more common application is in the calculation of statistical variance (or by extension, the standard deviation). The following formula is proposed as a parameter to describe the distribution of solidity within an open frame structure

$$\gamma_x = \frac{4 \cdot \sum_{i=1}^n \phi_i \cdot \left(\frac{x_i - \bar{x}}{L} \right)^2}{\sum_{i=1}^n \phi_i} \quad (9)$$

where the centroid, \bar{x} , is defined as

$$\bar{x} = \frac{\sum_{i=1}^n \phi_i \cdot x_i}{\sum_{i=1}^n \phi_i} \quad (10)$$

n = the number of elements along the x -axis. Example elements are frames and equipment elements.

ϕ_i = the solidity ratio of element, i , along the x -axis. The solidity of each element is the solid area of the element divided by the product of the height and width of the structure in the plane normal to the x -axis.

x_i = the distance of element, i , from the centroid, \bar{x} .

The bracketed term in the numerator of Eq. (9) is normalized by the length of the structure (along the x -axis) in order to eliminate overlap of coverage between this parameter, γ , and the parameter L/B . Eqs. (9) and (10) are divided by the cumulative solidity in order to eliminate overlap of coverage between γ and the solidity ratio, ϕ . The lower and upper limits of Eq. (9) are (0, 1). A value of zero corresponds to the case in which a structure of finite length, L , along the x -axis has all of its solidity concentrated at the centroid. This case is not possible and can only be approached, since a structure with such a concentration of solidity would be a single, plane frame or plate of negligible thickness oriented normal to the x -axis. Such a structure would have zero length, and Eq. (9) would therefore be undefined. A value of unity corresponds to the case of two plane frames or plates with negligible thickness oriented perpendicular to the x -axis and separated by some distance, L , along the x -axis. A value of 0.5 represents a structure with a completely uniform distribution of solidity along its length, L . Since the maximum value of the bracketed term in Eq. (9) is 0.5, the factor of four is required in order to set the maximum value of the parameter γ_x to one.

The variations of the maximum measured force coefficients, C_f , for the selected structures from Georgiou (1979) and Qiang's (1998) experiments were examined with respect to the solidity ratio, ϕ , the length to width aspect ratio, L/B , and the new parameter, γ , which describes the distribution of the structure's solidity along its length. For Georgiou's data set, C_f was found to increase with ϕ (although only two values of ϕ are represented in the selected data), increase with L/B , and decrease with γ . As such, a first order combination of these three dimensionless variables, $\phi \cdot (L/B) / \gamma$, was calculated for each model, and the maximum values of C_f were plotted against this parameter. Fig. 7 shows the results of this analysis for Georgiou's selected data. The data have collapsed quite well

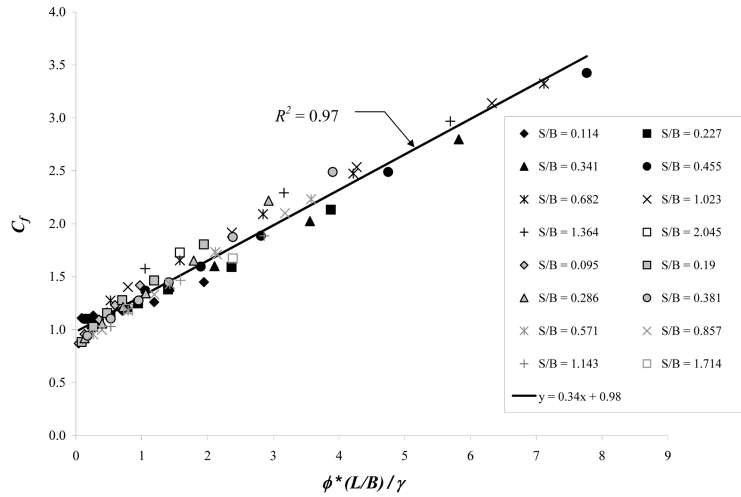


Fig. 7 Variation of maximum C_f with $\phi \cdot (L/B) / \gamma$ for selected models from Georgiou (1979). The term S/B corresponds to the spacing to width ratio of the parallel frames. The black and gray markers correspond to frames with $f = 0.77$ and 0.46 , respectively

for this combined parameter.

Conducting a similar exercise with Qiang’s data was not as straightforward. Qiang’s data did not collapse at all with $\phi \cdot (L/B) / \gamma$. It was subsequently found that the accumulated solidity [the denominator in Eqs. (9) and (10)] was more relevant than the projected solidity, ϕ . Accumulated solidity will be referred to as ϕ' , and is the summation of the solidity ratios of each frame or equipment plane perpendicular to the structural axis of interest. The difference between ϕ and ϕ' is that ϕ represents the projected solidity of the entire structure onto a single plane, whereas ϕ' represents the summation of the projected solidities of individual planes passing through the structure. Since there were only two L/B ratios present in Qiang’s data, any trend with this parameter was not well-represented. Finally, the variation of the measured maximum C_f with γ in Qiang’s data was weakly increasing. Fig. 8 shows that maximum measured C_f for Qiang’s selected data versus the combined parameter, $\phi' \cdot (L/B) \cdot \gamma$. This parameter increases as the structure becomes more solid (less porous), longer, and as the distribution of the solid areas are concentrated farther away from the center of the structure. The 200 series models correspond to models with height to width ratios (or elevation aspect ratios) of 2:1, plan aspect ratios of 1:1, and variable equipment and flooring configurations. The 1400 series models have height to width elevation aspect ratios of 1.5, length to width plan aspect ratios of 1.5, and variable equipment and flooring configurations. The G series models have the same envelope geometry as the 200 series, but with fixed equipment and variable front frame solidity. The 600 series models also have the same envelope dimensions as the 200 and G series models, but with fixed frame solidity and variable equipment solidity. As was the case for the comparisons with the analytical model, the differences in structure topology between Georgiou and Qiang’s studies has resulted in quite different behaviors for the aerodynamic coefficients.

For the more three dimensional models in Qiang’s experiments, the distribution of the solidity as measured by the parameter γ did not appear to be as important as it was in Georgiou’s experiments on multiple, parallel plane frames. Despite the high level of empirical correlation

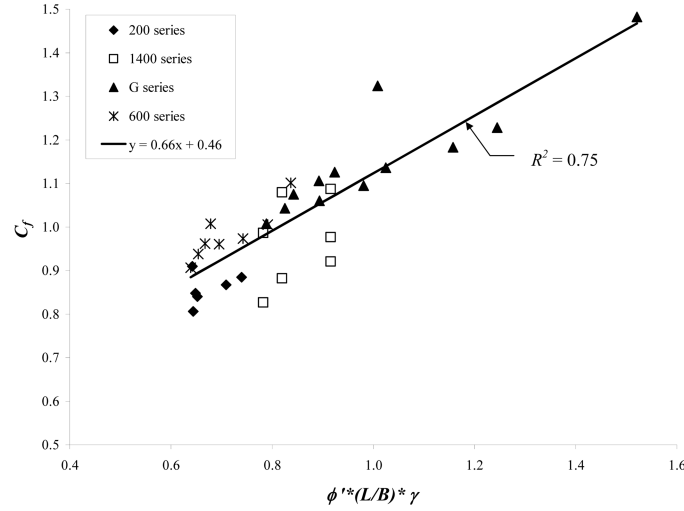


Fig. 8 Variation of maximum C_f with $\phi \cdot (L/B) \cdot \gamma$ for selected models from Qiang (1998)

that was found for Georgiou's selected data, there is limited practical application for the resulting relationships. Neither petrochemical structures nor unclad building frames would have such solidities for just the frames. Furthermore, open frames in petrochemical applications exist to house process equipment.

5. Upper limit force coefficient

The analysis in the preceding sections has clearly illustrated that the maximum force coefficient, C_f , for an open frame structure will increase continually with increasing L/B . This fact precludes the establishment of any universal upper limit for C_f for this category of structure. What remains, then, is the possibility of defining an upper limit C_f as a function of L/B . This possibility depends on the existence of an upper bound for the variable C_0 . It is reasonable to expect that such an upper bound on C_0 exists, since the alternative implies that an external flow in the neighborhood of a body with fixed L/B is capable of generating infinite force. For rectangular bodies with homogeneous porosity, the upper bound for C_0 is probably close to the value for an enclosed structure. This is not to say that the C_f for an enclosed structure of similar dimensions is the upper bound force coefficient. Eq. (8) indicates that C_f can increase indefinitely with L/B , regardless of the specified value of C_0 . The measured values of C_f for the models referenced in this paper all fell below the values defined by Eq. (8) with $\phi = 1.0$ and $C_0 = 1.4$.

How well the geometry of the model conforms to the assumption of homogenous porosity will affect the quality of the model prediction. For example, as the solidity of Georgiou's models increased, their geometry became more like parallel plates than a solid block. Previous research by the authors (Amoroso *et al.* 2010) has shown that an open frame structure with two parallel walls clad can experience much higher wind loads than an enclosed building with the same envelope geometry. Any attempt to define an upper bound C_f must respect these considerations.

6. Conclusions

This paper is concerned with the wind loading force coefficients (relative to body axes) for relatively solid, open frame industrial process structures. It is advantageous to work toward a general understanding of the wind loads on these structures, since accounting for the effects of each of the individual components becomes tedious and, most likely, less accurate as the structures become more densely occupied. Toward this end, an analytical model of the force coefficient was derived for porous structures. The force coefficient in this model was found to depend strongly on the length to width aspect ratio.

Comparisons of wind tunnel measurements for models consisting of multiple, parallel lattice frames and fully three-dimensional frameworks with the analytical model showed good agreement in the trends, a low bias and some scatter. The experimental data displayed the continual increase in force coefficient with increasing plan aspect ratio, L/B , which the analytical model predicts. On average, the analytical model predicted force coefficient values equal to 106% of the measured results. The coefficient of variation of the ratio of predicted force coefficient to measured force coefficient was 0.18.

In an attempt to address the issue of the scatter of the measurements with respect to the model predictions, another descriptive parameter was devised. This additional parameter described the distribution of the solidity within the model in a manner similar in concept to the second moment of area. This parameter was very effective in describing the variation of the force coefficients for multiple, parallel plane frame structures, but was less useful for three dimensional structures more representative of a petrochemical structure.

The possibility of establishing an upper bound force coefficient for open frame structures was discussed. For structures conforming to the geometric assumption of the analytical model derived in this paper, it is possible to describe the upper limit force coefficient only as a function of the plan aspect ratio. So in the purest sense, no such upper bound force coefficient exists for an open frame structure with arbitrary geometry. However, an upper bound can be defined as a function of L/B . This requires a selection of the empirical parameter C_0 (a baseline solid body force coefficient) which ensures that the results from the analytical model adequately envelope the force coefficient for porous structures. A selection of $C_0 = 1.4$ met this criteria for all of the experimental data examined in this study. It is the authors' opinion that Eq. (8), with a value of $C_0 = 1.4$, is appropriate for inclusion into wind loading codes, standards and guides for estimating wind loads for open-frame structures having projected solidity ratios greater than 50%.

References

- Amoroso, S.D., Hebert, K. and Levitan, M.L. (2010), "Wind tunnel tests for mean wind loads on partially-clad structures", *J. Wind Eng. Ind. Aerod.*, **98**(12), 689-700.
- Andrade, J.S., Costa, U.M.S., Almeida, M.P., Makse, H.A. and Stanley, H.E. (1999), "Inertial effects on fluid flow through porous media", *Phys. Rev. Lett.*, **82**(26), 5249-5252.
- ASCE (2006), *Minimum design loads for buildings and other structures*, SEI/ASCE 7-05 (ASCE Standard No. 7-05), American Society of Civil Engineers, Reston, VA.
- ASCE (1997), *Wind loads and anchor bolt design for petrochemical facilities*, Task Committee on Wind Induced Forces and Task Committee on Anchor Bolt Design, American Society of Civil Engineers, New York.
- Cook, N.J. (1990), *The designer's guide to wind loading of building structures. Part 2. static structures*, Building

- Research Establishment Report, Butterworths, London.
- ESDU (1980), *Blockage corrections for bluff bodies in confined flows*, ESDU Data Item 80024, Engineering Sciences Data Unit, ESDU International, London, UK.
- Georgiou, P.N. (1979), *A Study of the wind loads on building frames*, Masters Thesis, University of Western Ontario, Canada.
- Georgiou, P.N. and Vickery, B.J. (1979), "Wind loads on building frames", *Proceedings of the 5th International Conference on Wind Engineering*, Fort Collins, Colorado, USA, July.
- Letchford, C.W. (2001), "Wind Loads on rectangular signboards and hoardings", *J. Wind Eng. Ind. Aerod.*, **89**(2), 135-151.
- Levitan, M.L., Qiang, L. and Amoroso, S.D. (2004), "Wind tunnel tests on open-frame industrial/petrochemical structures", *Proceedings of the 5th International Colloquium on Bluff Body Aerodynamics and Applications*, Ottawa, Canada, July.
- Nadeem, A. and Levitan, M.L. (1997) "A refined method for calculating wind load combinations on open-framed structures", *J. Wind Eng. Ind. Aerod.*, **72**(1-3), 445-453.
- Qiang, L. (1998), *Wind tunnel tests for wind loads on open frame petrochemical structures*, Masters Thesis, Louisiana State University, Baton Rouge, LA.
- Richards, P.J. and Robinson, M. (1999), "Wind loads on porous structures", *J. Wind Eng. Ind. Aerod.*, **83**, 455-465.
- Standards Australia (2002), *Structural design actions, Part 2: wind actions*, Australian-New Zealand Standard, AS/NZS 1170.2:2002.
- Seifert, J., Li, Y.G., Axley, J. and Rösler, M. (2006), "Calculation of wind-driven cross ventilation in buildings with large openings", *J. Wind Eng. Ind. Aerod.*, **94**(12), 925-947.
- Yaragal, S.C., Ram, H.S.G. and Murthy, K.K. (2002), "Two-dimensional flow field behind perforated plates on a flat surface", *J. Wind Eng. Ind. Aerod.*, **90**(2), 75-90.
- Yaragal, S.C. (2004), "Unsteady 2-D flow field characteristics for perforated plates with a splitter", *Wind Struct.*, **7**(5), 317-332.